Impacts of geoengineering on regional terrestrial carbon cycles

Min Xu[1] Forrest M. Hoffman[1,2] Hyun Kang[1] Salil Mahajan[1] Cheng-En Yang[2] Xiaojuan Yang[1] Wei Zhang [1]

[1]Oak Ridge National Laboratory, Oak Ridge, Tennessee [2]University of Tennessee, Knoxville, Tennessee

Background and objectives

Injecting sulfur dioxide into the lower stratosphere as part of the stratospheric aerosol intervention (SAI) is considered to stabilize surface temperature without cutting emissions, and it aims to mitigate the strengthening of extreme events and wildfires caused by anthropogenic climate change. However, there are significant uncertainties regarding the effects of SAI on terrestrial and marine ecosystems, especially at regional scales. Moreover, gross primary productivity (GPP) and net biome productivity (NBP) generally represent the *photosynthetic capability* and *carbon sink strength* of ecosystems, the objectives of the study, therefore, are to investigate SAI impacts on regional terrestrial carbon cycles, specifically:

1. **study** and **compare** SAI impacts on GPP and NBP in the CMIP6 reference land regions simulated by two earth system models (CESM2 and E3SMv3) with a comprehensive chemistry mechanism and prognostic aerosol model under the high emission scenario (SSP5-8.5).
2. **identify** the main climate drivers to the changes of GPP caused by SAI at region scales.

Models and simulations

Two Earth System Models (ESMs):

- Energy Exascale Earth System Model (E3SM) version 3 coupled with the comprehensive Tropospheric, Stratospheric, Mesospheric, and Lower Thermospheric (TSMLT) chemistry model (E3SMv3-TSMLT)[1]
- Community Earth System Model version 2 (CESM2) with the Whole Atmosphere Community Climate Model (WACCM6)[2, 3]

Two simulations by the above two models:

- *Baseline*: SSP5-8.5 scenario of ScenarioMIP participated in the Coupled Model Intercomparison Project (CMIP6)
- *SAI*: 1.5°C peak shaving simulation (i.e., keeping the global surface temperature 1.5°C above the pre-industry level) under the SSP5-8.5 scenario following the same simulation protocol described by [3]

Table 1. Key schemes of CESM2-WACCM6 and E3SMv3-TSMLT

	CESM2-WACCM6	E3SMv3-TSMLT
Dynamic core	finite volume	spectral element
Horizontal resolution	0.95x1.25 for atmos. & land	ne30 (∼1.0x1.0) for atmos. 0.5x0.5 for land
Vertical levels	70	86
Model top	140 km (6×10^6 hPa)	80 km (0.01 hpa)
Radiation	RRTMG	RRTMG
Microphysics	MG2	P3
Aerosol	MAM4	MAM4/MAM5
Chemical solver	TSMLT	TSMLT
QBO	interactive	interactive
Land BGC	CLM5	ELM-CTC
Land use change	included	excluded*
Ocean	POP2	MPAS-O
Ocean BGC	MARBL (on)	BEC (off)
Injection scheme/height	feedback algorithm, 24 km	feedback algorithm, 24 km

*Since we focus our analysis on the differences between the SAI and baseline simulations, we anticipate that excluding land-use changes would not significantly affect results.

Latitudinal variations of SAI effects

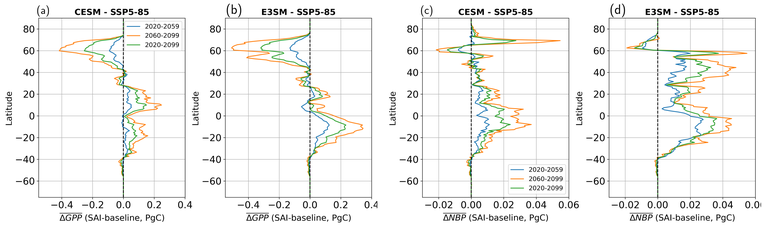

Figure 1. Latitudinal variations of GPP (a-b) and NBP (c-d) mean differences (SAI minus baseline, Unit: $PgCyr^{-1}$) under SSP5-8.5 during 2020-2059 (blue), 2060-2099 (orange) and 2020-2099 (green).

- Similar asymmetric patterns of the latitudinal distributions of GPP differences occur along latitudes in both CESM and E3SM, positive in the Northern tropics and Southern Hemisphere and negative in the high and middle latitudes.
- E3SM tends to simulate greater magnitudes of differences in GPP compared to CESM, specifically in the Southern Hemisphere's low-latitude regions and Northern Hemisphere's high-latitude regions.
- E3SM and CESM also diverge in their SAI's effects on NBP for the Northern Hemisphere's high and middle latitudes, with large positive NBP differences (>0.04 $PgCyr^{-1}$ during 2060-2099) in northern middle latitudes (30°N-60°N) for E3SM, and small positive differences (<0.005 $PgCyr^{-1}$ during 2060-2099) for CESM.

Geographic distributions of SAI effects

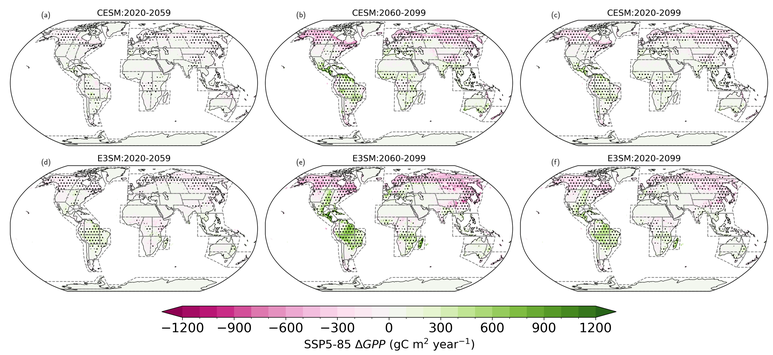

Figure 2. Mean GPP differences (Unit: $PgCyr^{-1}$) for the early 40 years (a,d, 2020-2059), the last 40 years (b,e, 2060-2099), and the full 80 years (c,f, 2020-2099) of the 21st century simulated by CESM (a-c) and E3SM (d-f) under SSP5-8.5. The hatched areas show the significance at a 95% confidence interval. The dash lines indicate the bounds of the CMIP6 reference regions[4].

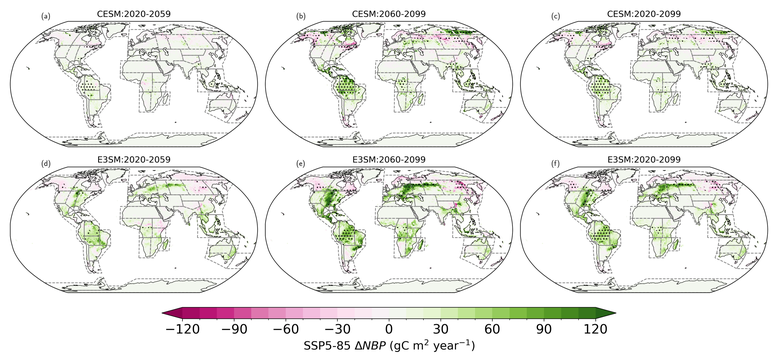

Figure 3. Same as above except for NBP.

Under SSP5-8.5, CESM and E3SM simulated similar geographic patterns of SAI effects on GPP, though E3SM shows larger magnitudes. The effects in the last 40 years are generally stronger than those in the first 40 years. For impacts on NBP, discrepancies were particularly notable in middle latitudes, with E3SM showing positive in central North America and northern Europe but negative in the Arctic and eastern Asia, contrasting with the CESM results.

SAI effects in CMIP6 reference regions [4]

Although the impact of SAI on the global ecosystem is generally less than 3% of the global GPP, it could affect GPP significantly from -87% to 62% of their regional GPP, and NBP from -4% to 8% at regional scales according to the E3SM results. For CESM, the SAI impacts at regional scales are -72% to 84% and -1.2% to 11% for GPP and NBP, respectively. Generally, the impacts of SAI on NBP simulated by E3SM are more significant than those simulated by CESM. In the three regions contributing most to global GPP (NSA, CAF, and SEA), SAI generally increases GPP and NBP while reducing AR, HR, or wildfire emissions. Moreover, several regions (i.e., NWS, WCE, SEAF, WSAF, WCA, EAU) significantly benefit from SAI, as it would lead to increases in GPP while decreases in HR and wildfire emissions.

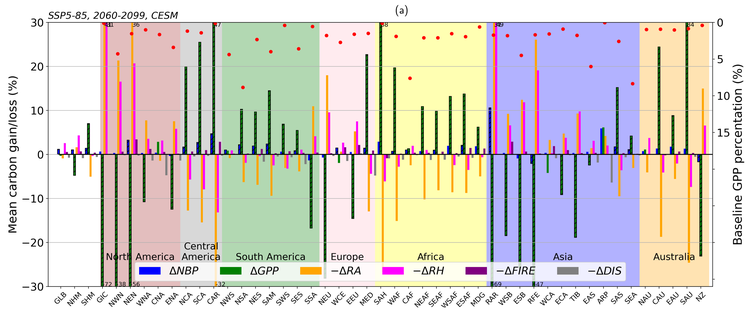

SAI effects in CMIP6 reference regions (cont'd)

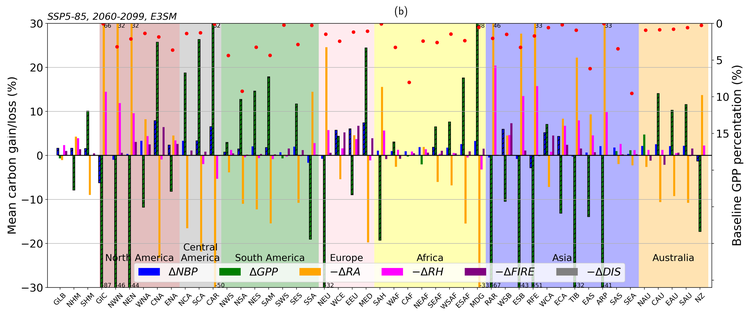

Figure 4. Mean differences (SAI minus baseline, Unit: %), normalized by the 10-yr mean regional GPP of baseline simulations from 2020 to 2029, of net biome productivity (ΔNBP), gross primary productivity (ΔGPP), autotrophic respiration ($-\Delta RA$), heterotrophic respiration ($-\Delta RH$), fire emission ($-\Delta FIRE$), and other disturbances ($-\Delta DIS$) during the last 40 years of the 21st century over SSP5-8.5 by CESM2-WACCM6 (a) and E3SMv3-TSMLT (b). Positive/negative values imply carbon gain/loss. The red dots of the top and right axes are the mean percentages of regional GPP over the global GPP of baseline simulations from 2020-2029.

Climate drivers of SAI effects under SSP5-8.5

Employing an extreme gradient boosting (XGB) model to reproduce the SAI effects on GPP simulated by CESM and E3SM and to identify the importance of six climate drivers, i.e., direct (R_{dir}) and diffuse (R_{dif}) radiation, vapor pressure deficit (VPD), temperature (T_{2m}), top 10cm soil water content (SWC), and precipitation (Pr).

Table 2. The first and second important climate drivers influencing the differences in mean GPP and NBP caused by SAI are illustrated in the selected regions across high, middle, and low latitudes. The importance of drivers is determined by applying the Shapley additive explanation (SHAP) method to the XGBoost regression models on the GPP differences. The 80-year cumulative GPP differences are also listed.

Latitude	Regions	R_{dir}		R_{dif}		VPD		T_{2m}		SWC		Pr		Cum. differences (PgC)	
		CESM	E3SM	CESM	E3SM	CESM	E3SM	CESM	E3SM	CESM	E3SM	CESM	E3SM	CESM	E3SM
High	NWN		√	√		√	√							-79	-97
	EEU		√	√		√	√							-15	-7
	WSB		√	√		√	√							-16	-11
Middle	CNA			√	√	√	√							5	39
	MED					√	√		√	√				25	17
	WCA			√	√	√	√							0	4
	EAS	√	√			√			√					-11	-60
Low	SCA	√				√	√				√			26	25
	NWS					√	√			√	√			2	11
	NSA					√	√			√	√			50	111
	SAM					√	√			√	√			42	81
	SES	√				√	√				√			19	34
	WAF					√	√			√	√			29	1
	CAF		√			√				√	√			3	-6
	SEAF						√			√		√	√	14	10
	SAS	√				√	√				√			27	0
	SEA					√	√			√			√	19	17

Conclusions

- SAI has a positive effect on NBP globally but a negative/positive impact on GPP in high-/low-latitude regions.
- E3SM and CESM simulate similar geographic distributions of SAI effects on GPP and NBP but differ in magnitude and specific regional impacts under SSP5-8.5. However, from 2060 to 2099, they exhibit distinct patterns in SAI's effects on NBP, likely due to differences in land biogeochemical process representations between the two models.
- The key climate drivers influencing GPP and NBP variability vary across latitude and between models.

Our results emphasize the regional differences and uncertainties in models and scenarios, highlighting the need for studies on SAI injection schemes and their effects on the regional carbon cycle.

Acknowledgement

This work was supported by the ORNL Laboratory Directed Research and Development (LDRD) program (LOIS: 10974) and the Reducing Uncertainties in Biogeochemical Interactions through Synthesis and Computation Scientific Focus Area (RUBISCO SFA), which are sponsored by the Climate and Environmental Sciences Division (CESD) of the Biological and Environmental Research (BER) Program in the U.S. Department of Energy (DOE) Office of Science. Analysis was performed on the Jupyterlab of the National Energy Research Scientific Computing Center (NERSC), a DOE Office of Science User Facility using NERSC award BER-ERCAP0029174. This research also used resources of the Oak Ridge Leadership Computing Facility (OLCF) at ORNL, which is supported by the DOE Office of Science under Contract No. DE-AC05-00OR22725. The Authors are grateful to ESGF and NCAR for providing CESM2-WACCM and its SAI results for downloading.

References

[1] H.-G. Kang, W. Zhang, S. Mahajan, M. Xu, F. M. Hoffman, C.-E. Yang, and X. Yang. A new configuration of e3smv3 for credible geoengineering simulations, in preparation.

[2] A. Gettelman, M. J. Mills, D. E. Kinnison, R. R. Garcia, A. K. Smith, D. R. Marsh, S. Tilmes, F. Vitt, C. G. Bardeen, J. McInerny, H.-L. Liu, S. C. Solomon, L. M. Polvani, L. K. Emmons, J.-F. Lamarque, J. H. Richter, A. S. Glanville, J. T. Bacmeister, A. S. Phillips, R. B. Neale, I. R. Simpson, A. K. DuVivier, A. Hodzic, and W. J. Randel. The Whole Atmosphere Community Climate Model Version 6 (WACCM6). 124(23):12380–12403.

[3] Simone Tilmes, Douglas G. MacMartin, Jan T. M. Lenaerts, Leo van Kampenhout, Laura Muntjewerf, Lili Xia, Cheryl S. Harrison, Kristen M. Krumhardt, Michael J. Mills, Ben Kravitz, and Alan Robock. Reaching 1.5 and 2.0 °C global surface temperature targets using stratospheric aerosol geoengineering. *Earth System Dynamics*, 11(3):579–601, July 2020.

[4] Maialen Iturbide, José M. Gutiérrez, Lincoln M. Alves, Joaquín Bedia, Ruth Cerezo-Mota, Ezequiel Cimadevilla, Antonio S. Cofiño, Alejandro Di Luca, Sergio Henrique Faria, Irina V. Gorodetskaya, Mathias Hauser, Sixto Herrera, Kevin Hennessy, Helene T. Hewitt, Richard G. Jones, Svitlana Krakovska, Rodrigo Manzanas, Daniel Martínez-Castro, Gemma T. Narisma, Intan S. Nurhati, Izidine Pinto, Sonia I. Seneviratne, Bart van den Hurk, and Carolina S. Vera. An update of IPCC climate reference regions for subcontinental analysis of climate model data: Definition and aggregated datasets. *Earth System Science Data*, 12(4):2959–2970, November 2020.